Root-Zone Warming Differently Benefits Mature and Newly Unfolded Leaves of *Cucumis sativus* L. Seedlings under Sub-Optimal Temperature Stress

Xiaozhuo Wang[☯], Weihua Zhang[☯], Yanxiu Miao, Lihong Gao*

Beijing Key Laboratory of Growth and Developmental Regulation for Protected Vegetable Crops, China Agricultural University, Beijing, China

☯ These authors contributed equally to this work.
* gaolh@cau.edu.cn

Abstract

Sub-optimal temperature extensively suppresses crop growth during cool-season greenhouse production. Root-zone (RZ) warming is considered an economical option to alleviate crop growth reduction. In this study we cultivated cucumber seedlings in nutrient solution under different air-RZ temperature treatments to investigate the effects of RZ warming on seedling growth- and photosynthesis-related parameters in leaves. The air-RZ temperature treatments included sub-optimal RZ temperature 13°C and sub-optimal air temperature 20/12°C (day/night) (S13), RZ warming at 19°C and sub-optimal air temperature (S19), and RZ warming at 19°C and optimal air temperature 26/18°C (day/night) (O19). In addition, for each air-RZ temperature treatment, half of the seedlings were also treated with 2% (*m/m*) polyethylene glycol (PEG) dissolved in nutrient solution to distinguish the effect of root-sourced water supply from RZ temperature. At the whole-plant level, S19 significantly increased the relative growth rate (RGR) by approximately 18% compared with S13, although the increase was less than in O19 (50%) due to delayed leaf emergence. S19 alleviated both diffusive and metabolic limitation of photosynthesis in mature leaves compared with S13, resulting in a photosynthetic rate similar to that in O19 leaves. In newly unfolded leaves, S19 significantly promoted leaf area expansion and alleviated stomatal limitation of photosynthesis compared with S13. PEG addition had a limited influence on RGR and leaf photosynthesis, but significantly suppressed new leaf expansion. Thus, our results indicate that under sub-optimal temperature conditions, RZ warming promotes cucumber seedling growth by differently benefiting mature and newly unfolded leaves. In addition, RZ warming enhanced root-sourced water supply, mainly promoting new leaf expansion, rather than photosynthesis.

Introduction

Low temperature is a prominent limiting factor for horticultural crop production in temperate regions, particularly during cool-season cultivation. Although chilling conditions can be largely avoided in heated or solar greenhouses, insufficient heating due to high fuel costs and/or long-term environmental considerations frequently result in sub-optimal temperature conditions, which usually persist for a long period [1,2]. Sub-optimal temperature stress usually leads to reduced vegetative growth, which may adversely affect yield and fruit quality [1]. Thus, to overcome the low-temperature imposed decrease of green-house plant production and to reduce energy consumption, environment control techniques that decrease heating costs, or raise crop resistance to unfavorable temperatures are required.

Root-zone (RZ) temperature regulation is a promising approach for maintaining plant health under sub-optimal temperatures [3,4], mainly because when compared with the aerial part, the RZ has a higher specific heat capacity and is more easily controlled [3,5]. Most importantly, a suitable RZ temperature is indispensable for plant health. Many studies have focused on the negative impacts of unfavorable RZ temperature on plant growth and physiological activities [6–11]. Improved production by applying root-warming/cooling methods has been reported in some field experiments [3–4,12–13]. However, most of the former studies were conducted under optimum air temperature conditions, and the specific effects of RZ temperature under unfavorable shoot temperature remain unclear.

One of the most remarkable effects induced by changing root temperature is the alteration of water uptake, which may have far-reaching implications. A number of studies have reported that a RZ temperature below the optimum decreases the water uptake ability of the root [7,14–17]. In addition, it has been demonstrated that decreased root-sourced water supply is strongly related to reduced leaf growth [10] and stomatal conductance [14,18], which will negatively affect the overall assimilation capability of a plant. However, it is still unclear how water uptake regulates plant growth under changes in root-zone temperature, because no study has investigated water uptake separate from other effects induced by root temperature conditions.

Despite the potential benefits of a so-called "non-stressful" RZ temperature for plants, negative effects may also occur. For example, Suzuki et al. [19] observed severe, visible leaf damage when chilled rice seedlings were provided with root warming at 25°C. The chilling injury was related to the blockage of photosynthetic electron transport, which was induced by the warm RZ temperature [20]. Soto et al. and Paredes et al. recently reported similar results [21,22]. Hao et al. observed that the activities of photosystem II (PSII) and antioxidant enzymes declined when heated peach seedlings were provided a non-stressful root temperature [23]. Because the interaction between roots and shoots under stressful conditions is complex and still unclear, the identification of a strategy for optimal environmental control was not as simple as expected in these studies. Therefore, further investigation of RZ temperature regulation is required to develop a deeper understanding of plant root-shoot communication and proper strategies for environmental control under non-optimal or stressful temperatures.

The objective of this study was to investigate the effects of RZ warming at a sub-optimal air temperature on growth characteristics and photosynthesis-related parameters in cucumber (*Cucumis sativus* L.) seedlings. The effect of water deficiency in the RZ temperature treatments was also estimated by adding polyethylene glycol (PEG), which is often used to simulate drought stress in hydroponic systems [24,25]. In this study, cucumber was used as a model species because cucumber is a major commercial crop that is sensitive to both low temperature and water stress [26,27].

Materials and Methods

Plant material and growth conditions

Cucumber (*Cucumis sativus* L. cv. Zhongnong No.16) seeds were pregerminated at 28°C for 26 hours, then sown onto hydroponic seedling-raising devices (Fig 1A) containing full-strength Yamazaki nutrient solution (pH was adjusted to approximately 6.0) [28] and cultured at 28°C for 30 hours. Germinated seedlings were then cultivated at day/night (10/14 h) temperatures of 26 /18°C and a relative humidity of 60–80% under photosynthetically active radiation (PAR) of approximately 100 μmol·m^{-2}·s^{-1}. On day 10 after germination, the seedlings were transplanted, with their hypocotyl and root in a 500-mL brown glass bottle (one seedling per bottle) containing nutrient solution. Bottles were placed in artificial light incubators (capacity: 430 L; RXZ-430E, Ningbo Jiangnan Instrument Factory, China) providing a daytime PAR of 250 μmol·m^{-2}·s^{-1} (fluorescent lamps, 6400K white) for five days. The RZ warming treatment began on day 16 after germination when each seedling had both a fully developed true leaf and a newly unfolded young leaf.

Root-zone treatments

On day 16 after germination, the bottles with seedlings were transferred to specially designed devices (Fig 1B) that could maintain different temperatures around both the shoots and roots of the seedlings. Each water bath tank was equipped with an electrothermal rod and connected to a semiconductor refrigerator (XH-LF162, XH-Electron, China) so that the solution temperature could be independently controlled. Air temperature was regulated by the light incubator itself.

There were three different temperature treatments. For the sub-optimal treatments, the air temperature was set at 20/12°C (day/night), and the water bath temperature (equivalent to the RZ temperature) was set at 13±1°C (abbreviated as S13) or 19±1°C (abbreviated as S19). For the optimal temperature treatments, the air temperature was set at 26/18°C (day/night), and the water bath temperature was set at 19±1°C (abbreviated as O19). Moreover, for each temperature treatment, half of the seedlings were also treated with 2% PEG dissolved in nutrient solution (S13+PEG, S19+PEG and O19+PEG). All treatments were continued until the second true leaf fully unfolded and the third leaf was just about to unfold, corresponding to a treatment period of 10 days for S13 (with or without PEG) and S19 (with or without PEG), and 5 days for O19 (with or without PEG). Forty seedlings per treatment were cultivated. On the last day of treatment, leaf gas exchange, Chl fluorescence and P700^{+} absorbance were measured. After the measurements, leaves were sampled for biochemical analyses. The remaining seedlings were used for growth characteristics analysis.

Air and RZ temperatures for each treatment were monitored and recorded by thermo recorders (RS-12 and RT-12, ESPEC MIC CORP., Japan; S1 Fig).

Bleeding rate

On day 4 after treatment, four seedlings per treatment were cut below the cotyledons and the incision was quickly covered with a tubelet filled with absorbent cotton to collect bleeding sap for 3 hours. The bleeding rate was calculated from the weight increment of the tubelets after this period [19,29].

Growth characteristics

Seedlings were harvested at both the beginning and end of the treatments (four replicates, four seedlings each replicate). All leaves were scanned (EPSON EXPRESSION 4990, Japan) and leaf
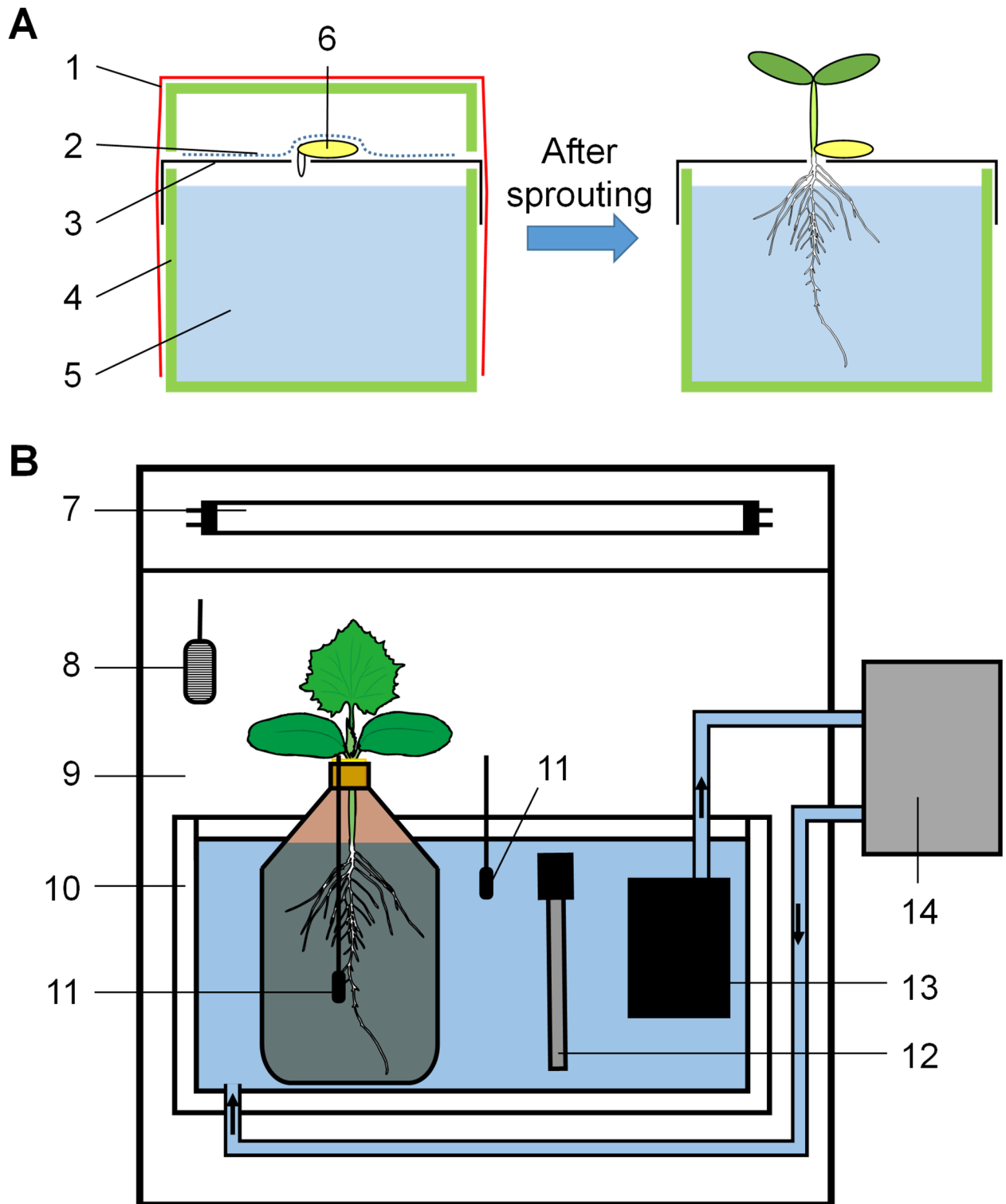
Fig 1. The scheme of cultivation devices used in this experiment. (A) The hydroponic seedling raising device: 1. plastic wrap; 2. moist paper towel; 3. perforated filter paper; 4. plastic box and its lid; 5. nutrient solution; 6. pregerminated cucumber seed; (B) The regulation system for air and root-zone (RZ) temperature: 7. fluorescent lamps; 8. air temperature thermocouple; 9. growth chamber; 10. polystyrene foam box; 11. water temperature thermocouple; 12. electrothermal rod; 13. circulating pump; 14. semiconductor refrigerator.

area was calculated with WinRHIZO software (LC4800-II LA2400; Sainte-Foy, Canada). Plant dry weight was recorded after drying in an oven at 85°C for 48 h. Growth parameters were calculated as follows [30]:

$$\text{RGR} = \frac{\ln W_2 - \ln W_1}{T_2 - T_1} \qquad (1)$$

$$\text{ULR} = \frac{W_2 - W_1}{T_2 - T_1} \cdot \frac{\ln L_{A2} - \ln L_{A1}}{L_{A2} - L_{A1}} \qquad (2)$$

$$\text{LAR} = \frac{L_{A2}/W_2 + L_{A1}/W_1}{2} \qquad (3)$$

$$\text{AGR} = \frac{W_2 - W_1}{T_2 - T_1} \qquad (4)$$

$$\text{SLA} = \frac{L_A}{W_L} \qquad (5)$$

RGR is the mean relative growth rate over the treatment interval. ULR is the mean unit leaf ratio (also called the "net assimilation rate", NAR). LAR is the mean leaf area ratio. AGR is the average growth rate over a treatment interval. SLA is the specific leaf area. W_1 and L_{A1} are the dry weight and leaf area at time T_1 (before treatment), W_2 and L_{A2} are the dry weight and leaf area at time T_2 (after treatment), and W_L is the dry weight of the same leaf.

Leaf gas-exchange parameters and chlorophyll content

Gas-exchange was measured on two true leaves (four cucumber seedlings per treatment) with an LI-6400xt gas exchange analyser (Li-Cor 6400xt, Lincoln, NE, USA). Determination of the net assimilation rate versus intercellular CO_2 concentration (A-C_i) curves started from the third hour of a light period. The temperature of the measurement chamber (the block temperature) was set at the air temperature of the corresponding treatment, and the PAR and air relative humidity were maintained at 1200 $\mu mol \cdot m^{-2} \cdot s^{-1}$ and 60%-70%, respectively. The reference CO_2 concentration was reduced from 400 to 320, 250, 200,150, 100 and 60 $\mu mol\ CO_2 \cdot mol^{-1}$, then increased from 60 to 400, 550, 750, 950, 1200 and 1500 $\mu mol\ CO_2 \cdot mol^{-1}$. The A-C_i curves were transformed to A-C_c curves (C_c: calculated CO_2 partial pressure at the sites of carboxylation [31]). The A-C_c curves were used to calculate the maximum rate of carboxylation (V_{cmax}) and the electron transport rate at saturating PPFD contributing to RuBP regeneration (J_{sat}), and then V_{cmax} and J_{sat} were calibrated to 25°C using software provided by Sharkey et al. [31]. The A-C_i (A-C_c) curves calibrated to 25°C were also used to calculate the photosynthetic rate limitations imposed by g_s (L_s) at C_a = 400 $\mu mol\ CO_2 \cdot mol^{-1}$ as described by ref. [32,33].

Leaf area was quickly scanned before chlorophyll (Chl) determination. After scanning, Chl was extracted by 95% ethanol and spectrophotometrically determined as described by Sartory and Grobbelaar [34].

Rubisco activity and its protein subunits abundance assay

Rubisco activity measurements and its protein subunits abundance assays were performed as previously described [35]. The leaves were harvested on the last day of the treatment, immediately frozen in liquid nitrogen, and stored at -80°C until further analysis.

The total soluble protein concentration was determined at 595 nm with bovine serum albumin as the standard according to the method of Bradford [36].

To determine the relative amounts of Rubisco large and small subunits, protein extracts were separated by 12% SDS-PAGE and transferred onto a PVDF membrane. For immunoblotting, both rabbit polyclonal anti-RbcL antibody (AS03 037, Agrisera, Vännäs, Sweden, 1:3000) and anti-RbcS antibody (AS07 259, Agrisera, Vännäs, Sweden, 1:3000) were used to detect proteins [37]. Second antibody (goat anti-rabbit, HRP-conjugated) was used at a dilution of 1:5000, and the signal was detected by SuperSignal West Pico Chemiluminescent Substrate (Thermo Fisher, US). For all treatments, the abundances of Rubisco large and small subunits were normalized to those in O19 leaves.

Chl fluorescence and P700$^+$ absorbance measurements

Chl fluorescence and P700$^+$ absorbance were measured with a Dual-PAM-100 system (Walz, Germany) [38] at the diurnal growth air temperature on two true leaves. Four cucumber seedlings from each treatment were used. After a night of dark adaptation and one hour of temperature adaptation, the minimum fluorescence (F_0) was determined, then two saturating pulses were applied to obtain the maximum fluorescence (F_m) and maximum P700$^+$ signal (P_m). After a 1-min dark period, actinic light (PAR = 221 μmol m^{-2} s^{-1}) was applied for 8 min, and saturating light pulses were applied every 20 s to determine the maximum fluorescence signal (F'_m) and maximum P700$^+$ signal (P'_m). A 1-s dark interval following each saturating pulse was used to determine the minimum level of P700$^+$ signal (P_0). The complementary quantum yields of PSII and PSI were calculated by Dual-PAM software [39–41] (Table 1). The electron transport rate (ETR) in the two photosystems was then calculated as indicated in Table 1.

The light induction transient of the Chl fluorescence (OJIP curve) was simultaneously recorded. Data in OJIP curves were converted to relative values as follows:

$$V_t = \frac{F_t - F_0}{F_m - F_0} \tag{6}$$

Where V_t and F_t represent the relative variable fluorescence and the fluorescence intensity at time t, respectively, and F_o and F_m denote the initial and the maximal fluorescence intensity, respectively. Further analysis of the OJIP curves, the so-called JIP-test, was conducted according to Strasser et al. [42–44]. Related glossary and formulas are provided in Table 1. All parameters were normalized using the corresponding values of O19 as reference, and then displayed in a radar map to more clearly depict the efficiencies for the whole energy cascade and the performance indexes [42].

Statistical methods

All data shown represent the mean of at least three repetitions. The data and the graphs were processed using Microsoft Excel 2013. For multiple comparisons, data were subjected to one-way analysis of variance (ANOVA) and the means were compared using Tukey HSD tests at $P = 0.05$ (software: IBM SPSS Statistics 19.0, IBM Corporation, NY, USA). Two-way ANOVA was performed to compare sources of variation, including RZ temperature (RT), polyethylene glycol (PEG), and the RT×PEG interaction.

Results

Bleeding rates under different temperature conditions

As shown in Fig 2, when compared with O19, S13 significantly decreased the bleeding rate of cucumber seedlings by a half, whereas S19 did not exhibit any influence. PEG addition limited

Table 1. Glossary and formulas of Chl fluorescence, P700$^+$ absorbance and the JIP-test parameters.

Biophysical parameters derived from Chl fluorescence and P700$^+$ absorbance parameters	
$\Phi_{II} = (F'_m - F)/F'_m$	Quantum yield of photochemical energy conversion in PSII
$\Phi_{NPQ} = F/F'_m - F/F_m$	Quantum yield of regulated non-photochemical energy loss in PS II
$\Phi_{NO} = F/F_m$	Quantum yield of non-regulated non-photochemical energy loss in PS II
$\Phi_I = (P'_m - P)/P_m$	Quantum yield of photochemical energy conversion in PSI
$\Phi_{ND} = (P - P_0)/P_m$	Quantum yield of non-photochemical quantum energy loss in PS I due to donor side limitation
$\Phi_{NA} = (P_m - P'_m)/P_m$	Quantum yield of non-photochemical quantum energy loss in PS I due to acceptor side limitation
$ETR_{II} = \Phi_{II} \times PAR \times 0.84 \times 0.5$	Electron transport rate in PSII
$ETR_I = \Phi_I \times PAR \times 0.84 \times 0.5$	Electron transport rate in PSI
Biophysical parameters derived from transient Chl fluorescence parameters	
$M_0 \equiv 4(F_{300\mu s} - F_{50\mu s})/(F_m - F_{50\mu s})$	Approximated initial slope (in ms^{-1}) of the fluorescence transient normalized on the maximal variable fluorescence F_V
$TR_0/ABS \equiv \varphi_{Po} = 1 - (F_0/F_m)$	Maximum quantum yield for primary photochemistry
$ET_0/TR_0 \equiv \Psi_{Eo} = 1 - V_J$	Efficiency/probability that an electron moves further than Q_A^-
$ET_0/ABS \equiv \varphi_{Eo} = [1 - (F_0 - F_m)](1 - V_J)$	Quantum yield for electron transport
$RE_0/ET_0 \equiv \delta_{Ro} = (1 - V_I)/(1 - V_J)$	Efficiency/probability with which an electron from the intersystem electron carriers is transferred to reduce end electron acceptors at the PSI acceptor side
$RE_0/ABS \equiv \varphi_{Ro} = [1 - (F_0/F_m)](1 - V_J)$	Quantum yield for reduction of end electron acceptors at the PSI acceptor side
$RC/ABS = \varphi_{Po}(V_J/M_0)$	Q_A reducing RCs per PSII antenna Chl
$PI_{ABS} = RC/ABS \cdot \frac{\varphi_{Po}}{1 - \varphi_{Po}} \cdot \frac{\psi_{Eo}}{1 - \psi_{Eo}}$	Performance index (potential) for energy conservation from photons absorbed by PSII to the reduction of intersystem electron acceptors
$PI_{total} = PI_{ABS} \cdot \frac{\delta_{Ro}}{1 - \delta_{Ro}}$	Performance index (potential) for energy conservation from photons absorbed by PSII to the reduction of PSI end acceptors

Subscripts J and I denote J-step (2 ms) and I-step (30 ms) of OJIP, respectively.

doi:10.1371/journal.pone.0155298.t001

the bleeding rate in O19 and S19 to a similar extent as S13. Thus, a decrease of 6°C in RZ temperature (S13 versus S19 and O19) and 2% PEG addition exhibited similar effects on limiting the bleeding rate in this experiment.

Plant growth parameters under different temperature conditions

Compared with O19, the overall suboptimal temperature significantly decreased plant RGR (S13 with or without PEG addition, Fig 3A). Compared with S13, RZ warming (S19) significantly increased RGR by approximately 18%. However, PEG did not influence RGR ($P > 0.05$).

The RGR can be divided into two parts: ULR and LAR (Fig 3A). ULR was not influenced by temperature treatments in the absence of PEG but significantly increased in O19 and S19 treatments compared with S13 in the presence of PEG. LAR was significantly increased by S19 compared with S13, and by O19 compared with S19 in the absence of PEG. However, for all temperature treatments, PEG addition significantly decreased LAR, suggesting that the morphological characteristics of leaves are influenced by either RZ temperature or PEG addition.

In this experiment, two true leaves of each seedling were observed separately: the first true leaf, which was nearly mature before treatment, and the second true leaf, which was about to expand when the treatment started. These two leaves responded differently to different temperatures. The difference in leaf area induced by treatments was greater in the second leaf than in the first leaf (Fig 3B). Leaf area growth rates are shown in Fig 3C. The two true leaves grew more slowly under sub-optimal temperature conditions. For the first leaf, area growth was generally less evident during treatment compared to the newly unfolded leaf. The leaf area growth
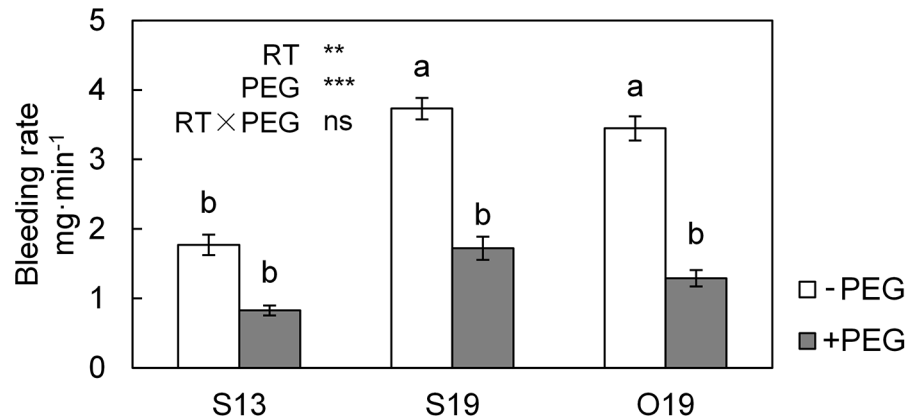
Fig 2. The bleeding rate of seedlings under different root-zone (RZ) conditions. All data are presented as means ± standard error (n = 3). Means with different letters denote significant difference ($P < 0.05$) by Tukey HSD. Source of variation: root-zone temperature (RT), polyethylene glycol (PEG), and RT×PEG interaction. ** $P < 0.01$; *** $P < 0.001$; ns: not significant.

doi:10.1371/journal.pone.0155298.g002

rate of seedlings in O19 was significantly higher than that in any other treatment. The area growth rate of the second leaf was significantly improved by increasing the RZ temperature; the increase was nearly two fold in S19 and more than threefold in O19 treatment compared with S13. However, the addition of PEG counteracted this effect in S19 and O19, as shown in Fig 3C, and a significant decrease in the leaf area growth rate was observed in S13 in the presence of PEG. With respect to the dry mass increment, compared with S13, S19 did not affect AGR of the first leaf, but significantly increased AGR of the second leaf to the level of O19 (Fig 3C). PEG treatments increased the mean AGR of the first leaf in each temperature treatment (significantly in S19), but significantly decreased the AGR of the second leaf in the seedlings exposed to both S13 and S19 treatments. Because PEG had no significant influence on RGR (Fig 3A), restricted expansion of the second leaf may lead to allocation of new dry mass mainly to other organs, such as the first leaf. RZ warming did not influence SLA of the first leaf but significantly increased SLA of the second leaf in S19 compared with S13 (Fig 3C). In all treatments, PEG addition significantly decreased SLA of the true leaves, except for the first leaf of S19 seedlings. The observed variation of SLA can be used to compare the effect of all treatments on leaf area with leaf weight. Thus, the above results indicate that in the second leaf, the positive effect of RZ warming and the negative effect of PEG addition were stronger for leaf area than for leaf weight.

Photosynthetic parameters under different temperature conditions

In the first true leaf, the net CO_2 assimilation rate (A_{400}) was low when seedlings were maintained in an overall sub-optimal temperature environment (S13, Table 2). However, A_{400} was significantly increased by RZ warming (S19 versus S13) and reached the levels measured under optimal conditions (O19). V_{cmax} and J_{sat}, which partially represent non-stomatal limitation of leaf photosynthesis, exhibited similar trends as A_{400}, indicating that both the dark and light reactions of photosynthesis were promoted by RZ warming treatment (S19 versus S13). The extent of stomatal limitation was also evaluated (g_s, C_i and L_s). Severe stomatal closure was observed in overall sub-optimal temperature-treated seedlings (S13), leading to high L_s and a low Tr. This negative condition was partially alleviated by RZ warming (S13 versus S19 and O19). The lack of a significant difference in C_i between S19 and S13 seedlings indicates that non-stomatal and stomatal limitation were alleviated to a similar extent by S19. PEG
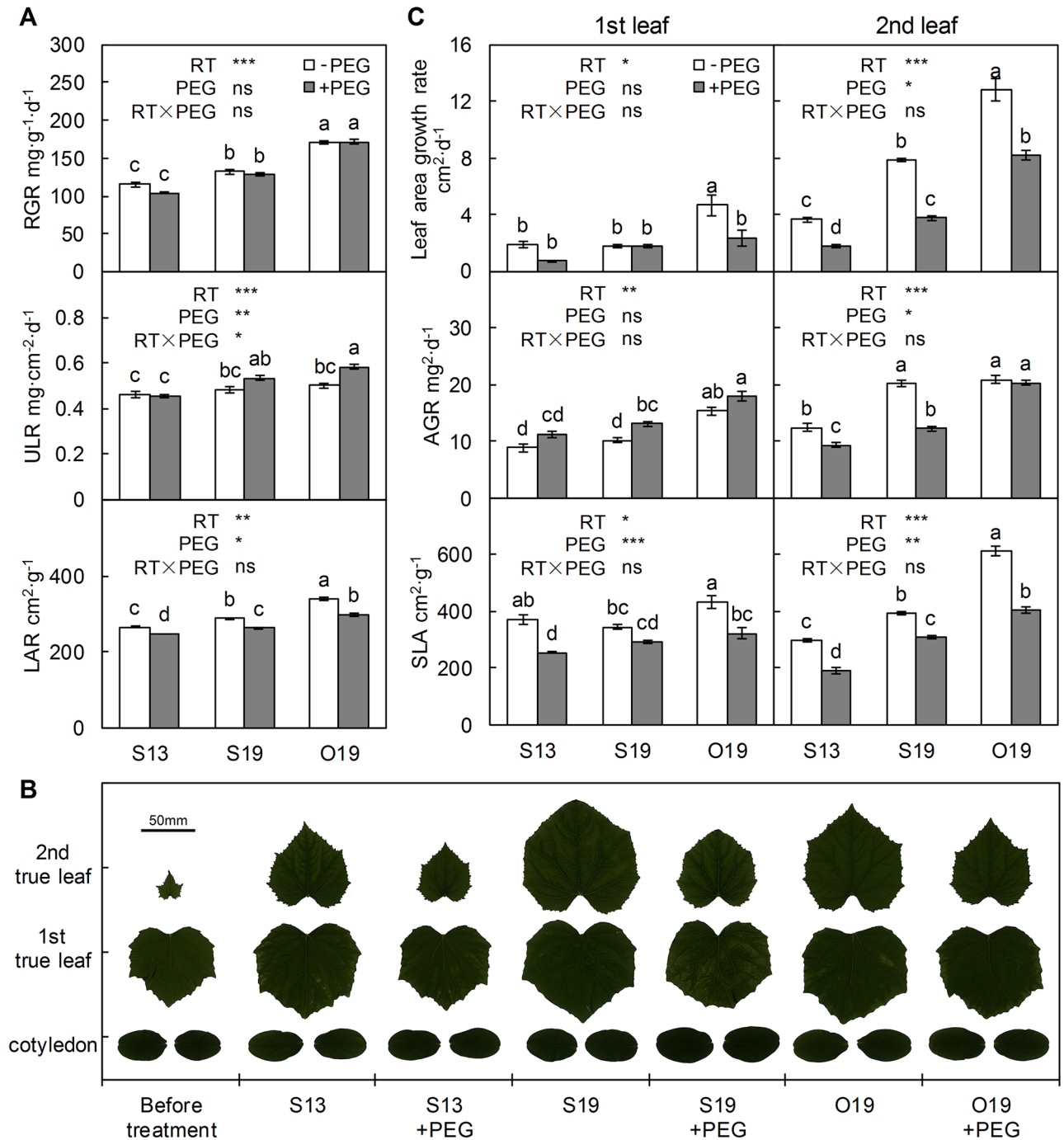
Fig 3. Plant growth characteristics under different root-zone (RZ) temperature and PEG treatments. (A) Relative growth rate (RGR) of the total dry mass, unit leaf rate (ULR) and leaf area ratio (LAR). (B) Scanned images of leaves. (C) Leaf area growth rate, dry mass average growth rate (AGR) and specific leaf area (SLA) of the 1st leaf and 2nd leaf. Means ± standard error are presented (n = 4). Means with different letters are significantly different ($P < 0.05$) by Tukey HSD. Source of variation: RZ temperature, RT; polyethylene glycol, PEG; and RT×PEG interaction; * $P < 0.05$; ** $P < 0.01$; *** $P < 0.001$; ns: not significant.

Table 2. Gas-exchange parameters in the two true leaves of cucumber seedlings under different root-zone (RZ) temperature and PEG treatments.

Treatment	A_{400} µmol CO_2·m^{-2}·s^{-1}		V_{cmax} µmol·m^{-2}·s^{-1}		J_{sat} µmol·m^{-2}·s^{-1}		g_s mol H_2O·m^{-2}·s^{-1}		C_i µmol·mol^{-1}		L_s		Tr mmol H_2O·m^{-2}·s^{-1}	
1st leaf														
S13	6.2	c	45	b	99	d	0.05	b	281	c	0.38	a	0.76	c
S13+PEG	4.7	c	41	b	103	cd	0.06	b	320	ab	0.32	ab	0.41	c
S19	17.6	a	78	a	141	a	0.13	ab	267	c	0.27	bc	1.50	b
S19+PEG	12.9	b	52	b	121	b	0.13	ab	297	bc	0.23	c	1.52	b
O19	18.4	a	71	a	119	bc	0.25	a	316	ab	0.09	d	2.88	a
O19+PEG	16.5	a	67	a	122	b	0.26	a	336	a	0.13	d	1.96	b
Source of variation														
RT	0.000		0.000		0.000		0.003		0.493		0.000		0.000	
PEG	0.007		0.010		0.873		0.918		0.032		0.607		0.134	
RT×PEG	0.288		0.151		0.387		0.831		0.387		0.432		0.654	
Adjusted R^2	0.927		0.844		0.589		0.338		0.145		0.546		0.636	
2nd leaf														
S13	9.6	c	50	bc	107	a	0.07	cd	270	b	0.33	ab	0.83	b
S13+PEG	4.0	d	35	d	83	c	0.03	d	277	b	0.43	a	0.42	b
S19	13.0	b	45	cd	85	bc	0.19	b	328	a	0.14	cd	1.88	a
S19+PEG	12.3	b	48	cd	101	abc	0.13	c	289	b	0.23	bc	1.01	b
O19	16.9	a	66	a	104	ab	0.28	a	339	a	0.05	d	2.39	a
O19+PEG	16.9	a	60	ab	110	a	0.26	ab	336	a	0.11	d	2.41	a
Source of variation														
RT	0.000		0.015		0.045		0.000		0.000		0.000		0.000	
PEG	0.007		0.759		0.660		0.161		0.528		0.010		0.126	
RT×PEG	0.013		0.328		0.021		0.946		0.166		0.647		0.972	
Adjusted R^2	0.799		0.233		0.318		0.621		0.640		0.792		0.572	

Net CO_2 assimilation rate at C_a = 400 µmol·mol^{-1} (A_{400}); maximum rate of carboxylation (V_{cmax}); electron transport rate at saturating PPFD (J_{sat}); stomatal conductance (g_s); intercellular CO_2 concentrations (C_i) at C_a = 400 µmol·mol^{-1}; relative limitation posed by stomatal conductance (L_s) and transpiration rate (Tr). All data except g_s and Tr, were calibrated to 25°C estimated from A/C_c curves. Means with different letters are significantly different ($P < 0.05$, n = 3 or 4) by Tukey HSD. Source of variation: P values of root-zone temperature (RT), polyethylene glycol (PEG) and RT×PEG interaction.

doi:10.1371/journal.pone.0155298.t002

treatments exhibited a smaller influence on photosynthesis than RZ temperature, and almost no effect on stomatal conductance or transpiration rate (except O19), although there was a non-significant trend in which PEG addition increased C_i and decreased L_s, indicating that PEG addition might result in greater non-stomatal limitation than stomatal limitation.

In the second true leaf, S19 had no positive effect on V_{cmax} and J_{sat} compared with S13 but promoted g_s and A_{400}. The increase in C_i (S19 versus S13) induced by RZ warming indicates the alleviation of stomatal limitation in the second leaf. PEG treatment differently influenced photosynthesis in the second leaf in S13, S19 and O19 seedlings. In S13+PEG seedlings, the development of the second leaf was extremely suppressed, as shown in Fig 3B, and its A_{400} decreased mainly due to the low V_{cmax} and J_{sat}. In S19+ PEG seedlings, the decrease in A_{400} was more due to stomatal limitation (g_s and L_s, Table 2), similar to S13 seedlings; in O19+PEG seedlings, A_{400} was not affected. The transpiration rates of the second leaf showed similar trends with g_s in all the treatments.

Data on Rubisco activity and amount are presented in Table 3. In the first true leaf, the initial and total Rubisco activity exhibited similar trends, these parameters increased in the order

Table 3. Rubisco properties, total chlorophyll and soluble protein in cucumber seedling leaves under different root-zone (RZ) temperature and PEG treatments.

Treatment	Rubisco initial activity µmol·g⁻¹ protein·⁻¹min*	Rubisco total activity µmol·g⁻¹ protein·⁻¹min	Rubisco activation rate %	Rubisco large subunits relative abundance	Rubisco small subunits relative abundance	Total Chl µg·cm⁻²	Total soluble protein mg·g⁻¹FW
1st leaf							
S13	208(63) c	251(67) c	83.0% a	1.39 a	1.56 a	36.7 bc	18.9 a
S13+PEG	199(60) c	243(64) c	81.6% a	1.37 a	1.38 a	32.6 c	17.9 a
S19	275(84) ab	327(87) b	84.0% a	1.58 a	1.62 a	46.6 a	18.8 a
S19+PEG	255(78) bc	300(80) b	84.9% a	1.45 a	1.40 a	47.3 a	20.8 a
O19	329(100) a	377(100) a	87.0% a	1.85 a	1.91 a	51.6 a	19.7 a
O19+PEG	296(90) ab	340(90) ab	87.0% a	1.52 a	1.47 a	43.3 ab	20.8 a
Source of variation							
RT	0.000	0.000	0.110	0.102	0.255	0.000	0.039
PEG	0.131	0.195	0.695	0.348	0.095	0.106	0.474
RT×PEG	0.229	0.347	0.871	0.473	0.903	0.616	0.464
Adjusted R²	0.742	0.668	0.004	0.125	0.120	0.585	0.167
2nd leaf							
S13	225(83) bc	310(93) ab	72.6% ab	1.83 a	1.67 a	45.0 a	24.6 a
S13+PEG	191(71) c	268(80) b	71.1% b	1.57 a	1.50 a	20.0 c	15.2 c
S19	236(87) ab	318(95) a	74.0% ab	1.61 a	1.79 a	42.2 ab	19.7 b
S19+PEG	224(83) bc	314(94) a	71.4% ab	1.80 a	1.83 a	38.5 ab	20.7 b
O19	270(100) a	334(100) a	81.0% a	1.84 a	1.78 a	41.9 ab	20.4 b
O19+PEG	273(101) a	346(104) a	79.2% ab	1.65 a	1.72 a	34.6 b	21.0 b
Source of variation							
RT	0.005	0.003	0.041	0.590	0.124	0.000	0.350
PEG	0.051	0.125	0.599	0.634	0.239	0.000	0.000
RT×PEG	0.033	0.126	0.802	0.630	0.819	0.000	0.000
Adjusted R²	0.453	0.421	0.116	-0.150	0.069	0.878	0.747

Means with different letters are significantly different ($P < 0.05$, n = 3 or 4) by Tukey HSD. Source of variation: P values of root-zone temperature (RT), polyethylene glycol (PEG) and RT×PEG interaction.

*: the numbers in parentheses indicate the percentages of the control (O19).

doi:10.1371/journal.pone.0155298.t003

S13<S19<O19. The Rubisco activation rate did not differ significantly among the different treatments. The translation of both the large and small subunits of Rubisco was reduced at sub-optimal air temperature; however, RZ warming did not significantly change these parameters. In the second true leaf, neither the activity nor amount of Rubisco was influenced by RZ warming under sub-optimal temperature conditions. The relative values of the initial and total Rubisco activities in the sub-optimal temperature treatments were higher in the second true leaf than in the first true leaf, indicating acclimation in the second true leaf. Similarly, when comparing S13 seedlings with S19 and O19 seedlings, the total chlorophyll was significantly lower in the mature leaf but unchanged in the newly unfolded leaf. Likewise, the soluble protein was not different in the mature leaf but significantly higher in the newly unfolded leaf. PEG treatment usually resulted in no effect or a slightly negative effect on the biochemical parameters in both leaves, except in the second leaf of S13+PEG seedlings, in which Chl and protein concentration were significantly reduced.

Due to the apparent acclimation of photosynthetic non-stomatal limitation in the second true leaf of S13 seedlings, in the following results, the reported data are solely from the first true leaf unless otherwise stated. The data for the second true leaf are provided in the supporting information (S1 and S2 Tables).

Chl fluorescence and P700$^+$ level under different temperature conditions

Sub-optimal temperature induced a low electron transport rate of the two photosystems in the first true leaf (S13 versus O19, Fig 4). S19 significantly increased ETR$_{II}$ and ETR$_I$ by 50% and 40%, respectively, compared with S13. ETR$_I$ / ETR$_{II}$ was 1.34, 1.25, and 1.24 in S13, S19 and O19 seedlings, respectively, and did not differ significantly. In PSII, Φ_{NPQ} did not change in S19 compared with S13, whereas Φ_{NO} significantly decreased in S19 to the level in O19, indicating less excess energy. As for PSI, Φ_{ND} in S19 seedlings was only 58% of that in S13, whereas
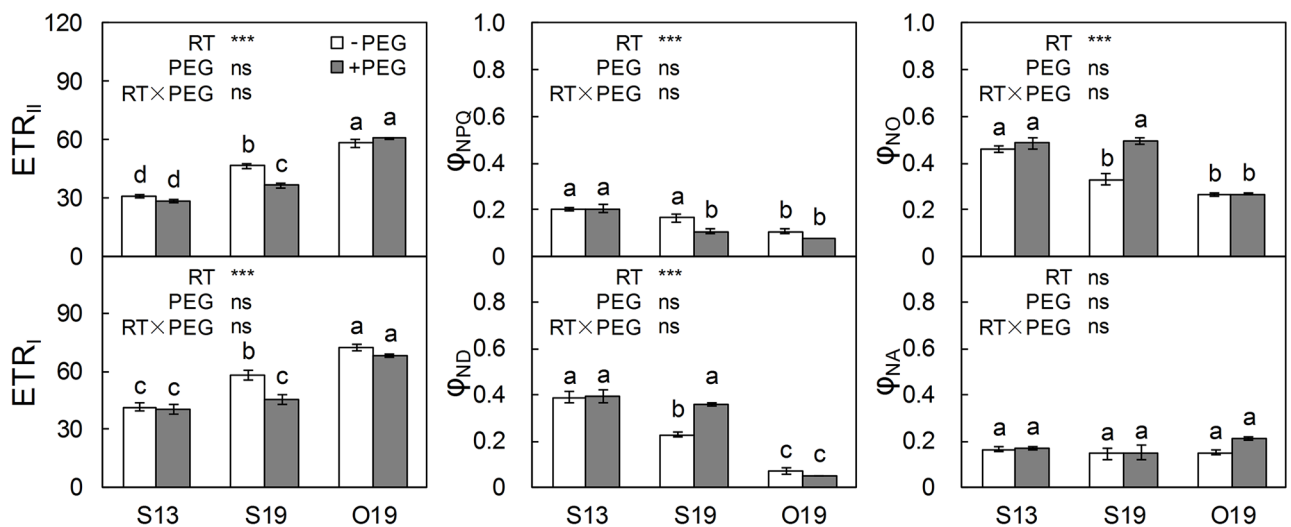

Fig 4. Chl fluorescence and P700$^+$ parameters in the first true leaves under different root-zone (RZ) temperature and PEG treatments. Electron transport rate of PSII (ETR$_{II}$), quantum yield of light-induced non-photochemical fluorescence quenching (Φ_{NPQ}) of PSII and quantum yield of non-light-induced non-photochemical fluorescence quenching (Φ_{NO}); electron transport rates of PSI (ETR$_I$), quantum yield of non-photochemical energy dissipation in PSI due to donor-side limitations (Φ_{ND}) and quantum yield of non-photochemical energy dissipation in PSI due to acceptor-side limitations (Φ_{NA}). Means ± standard error are presented (n = 3 or 4). Means with different letters are significantly different ($P < 0.05$) by Tukey HSD. Source of variation: root-zone temperature, RT; polyethylene glycol, PEG; and RT×PEG interaction; *** $P < 0.001$; ns: not significant.
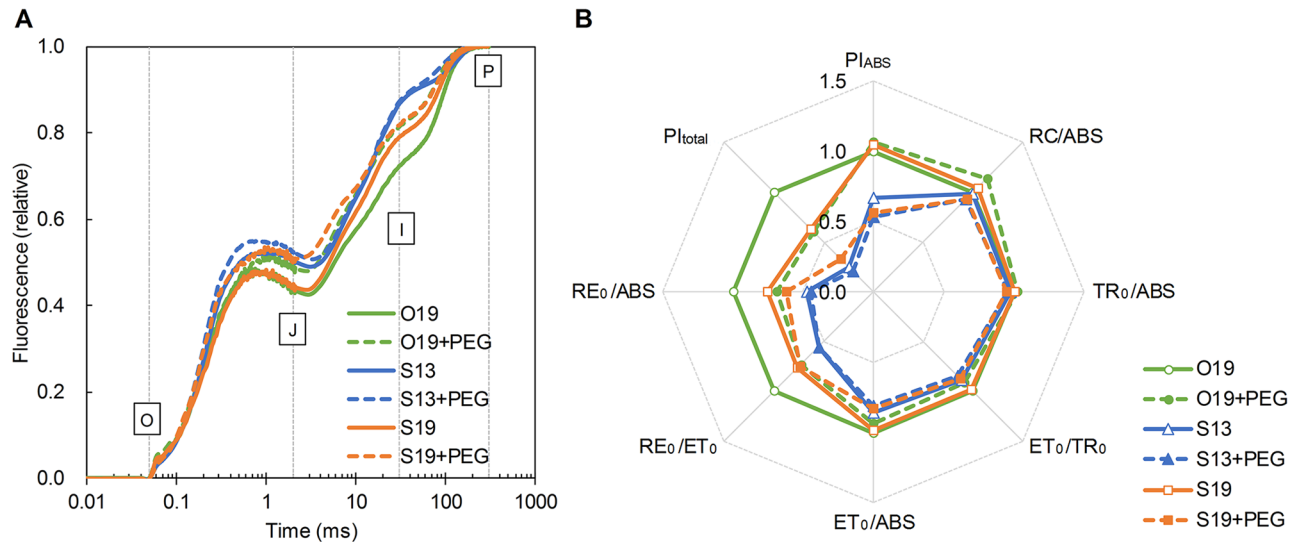
Fig 5. Light induction curves of transient Chl fluorescence (A) and JIP-test results (B). Data were determined in the first true leaves of cucumber seedlings under different root-zone (RZ) temperature and PEG treatments. RC/ABS: Q_A reducing RCs per PSII antenna Chl; TR_o/ABS: maximum quantum yield for primary photochemistry; ET_o/TR_o: efficiency/probability that an electron moves further than Q_A^-; ET_o/ABS: quantum yield for electron transport; RE_o/ET_o: efficiency/probability with which an electron from the intersystem electron carriers is transferred to reduce end electron acceptors at the PSI acceptor side; RE_o/ABS: quantum yield for reduction of end electron acceptors at the PSI acceptor side; PI_{ABS}: performance index (potential) for energy conservation from photons absorbed by PSII to the reduction of intersystem electron acceptors; PI_{total}: performance index (potential) for energy conservation from photons absorbed by PSII to the reduction of PSI end acceptors. Lines and values are the averages of four individual measurements with four different seedlings.

doi:10.1371/journal.pone.0155298.g005

Φ_{NA} exhibited no obvious difference among all treatments, indicating that PSI was limited mainly at the donor side. PEG treatment reduced most of the fluorescence parameters of S19 seedlings to the level of S13 but had no effect on either S13 or O19 seedlings.

Light induction of Chl fluorescence transient and JIP-test parameters under different temperature conditions

Chl fluorescence induction curves (OJIP curves, Fig 5A) were recorded to investigate the location at which electron transport was blocked between PSII and PSI. The high J-level and I-level in S13 seedlings were decreased by RZ warming under sub-optimal temperature conditions (S19 versus S13), and the I-level was further decreased by O19. Adding PEG generally increased both the J-level and I-level in all temperature treatments. The JIP-test parameters were derived from quantitative analysis of the OJIP curves (Fig 5B). RC/ABS and TR_0/ABS were not significantly different among the temperature treatments. Compared with S13, S19 significantly increased the efficiency parameters (ET_0/TR_0 and RE_0/ET_0) and, consequently, quantum yields (ET_0/ABS and RE_0/ABS). These increases in S19 resulted in a PI_{ABS} similar to O19 and a PI_{total} of 64% relative to O19, indicating significantly improved overall performance compared with S13 (67% and 25%, respectively). PEG addition did not affect S13 seedlings but inhibited PI_{ABS} and PI_{total} by decreasing ET_0/TR_0 in S19 seedlings and inhibited PI_{total} by decreasing both ET_0/TR_0 and RE_0/ET_0 in O19 seedlings.

Discussion

In general, sub-optimal temperature suppresses plant growth by influencing both morphological properties and physiological activity of the leaves [1,45,46]. In this experiment, an

increment of 6°C in RZ warming treatment (S13 versus S19) had a significant positive effect on the growth of cucumber seedlings (RGR, Fig 3A). This not only preserved the photosynthetic capability of the already existing leaf but also promoted the expansion rate of the newly developed leaf (Table 2 and Fig 3C). However, the phenology of the seedlings was not influenced by RZ temperature. It required 10 days for the second true leaf to fully unfold in sub-optimal air temperature treatments, but only 5 days in the optimal air temperature treatments. The negligible contribution of RZ warming to new leaf emergence may be the main reason that the RGR was lower in S19 seedlings than in O19 seedlings (Fig 3A). However, RZ warming obviously promoted new leaf expansion (Fig 3B).

Root-zone temperature regulation always leads to simultaneous changes in the root-sourced water supply [10,16,19], but differentiating the roles of root-sourced water signals and temperature signals is difficult. We provided a rough solution to this problem in this experiment by adding PEG to decrease the bleeding rate of S19/O19 seedlings to a level similar to that in S13 seedlings (Fig 2). The failure of PEG addition to influence RGR indicates that the improved root water availability at warmer RZ temperature did not affect total biomass accumulation. By contrast, PEG addition decreased the LAR and the growth rate of the newly unfolded leaf in S19 seedlings to a level similar to that in S13 seedlings (Fig 3A and 3C). The slight artificial water stress also decreased new leaf expansion in S13 and O19+PEG seedlings. These results are consistent with the work of Poire et al. [10], who observed that leaf expansion of *Ricinus communis* was strongly inhibited at a low RZ temperature during the day; they hypothesized that the decreased water supply due to root-cooling played a leading role. Similar results were also observed in rice plants [47], the leaf area expansion and transpiration were simultaneously reduced by 13°C root temperature.

PEG addition also provided insights on the ULR results. ULR did not differ significantly between S19 and S13 seedlings, indicating equilibria of the suppression / promotion of both total leaf area and total biomass accumulation in RZ warming. However, in S19+PEG seedlings, where the effect of water supply was excluded via the addition of PEG to isolate the effect of temperature, the ULR was significantly higher than in S13 seedlings. As shown in Fig 3B and 3C, the leaf area was similar in S19+PEG and S13 seedlings, and thus the increment of ULR in S19+PEG seedlings was mainly due to increased total biomass accumulation. This result further indicates that a warm RZ temperature itself rather than the improved root-sourced water supply can increase the net assimilation rate. This inference is also supported by the negligible effects of PEG on RGRs.

A number of studies have demonstrated that unfavorable RZ temperature depresses photosynthesis under normal air temperature conditions [9,48–51]. In this experiment, for the newly unfolded leaf, the photosynthetic activity of S13 seedlings was suppressed mainly due to stomatal limitation (Table 2), rather than metabolic limitation (V_{cmax} and J_{sat} in Table 2, Rubisco-related parameters in Table 3, and S1 and S2 Tables). Thus RZ warming treatment exhibited no significant benefits for this aspect. Similar acclimation of photosynthesis has been observed in Arabidopsis leaves developing at 5°C and was attributed to increases of available phosphates and the activity of several Calvin-cycle and sucrose-synthesis related enzymes [52]. A low RZ temperature alone may have also contributed to acclimation in a study by Venzhik et al. [51] in which wheat leaves exhibited decreased leaf area but increased cold tolerance after exposure to 2°C root chilling. Thus we suggest that for newly unfolded leaves during sub-optimal temperature stress, RZ warming benefits photosynthetic ability mainly via stomata opening rather than metabolic processes such as Rubisco carboxylation activity and electron transport rate.

Photosynthetic activity was severely impaired in the first leaf after transfer to a sub-optimal environment from an optimal temperature environment. Increasing the RZ temperature by 6°C (S19) maintained A_{400} at the high level of O19 (Table 2) by alleviating both stomatal and

non-stomatal limitation (S19 seedlings versus S13). Stomatal apertures can be finely modulated by various environmental conditions such as hormonal stimuli, light signals, water status, CO_2, and air temperature [53,54]. Non-optimal RZ temperature is also considered a cause of stomatal closure [14,49,55]. In addition to water supply, signals from the root such as ABA (abscisic acid) have also been identified as playing an important role in studies of RZ temperature [23,56]. For instance, Zhang et al. [50] demonstrated that in six *Cucurbitaceae* species at ambient air temperature, the change in the net photosynthesis rate was mainly due to the change in g_s, which was regulated by RZ temperature via root-sourced ABA. In our experiment, additional PEG treatment had a very limited effect on g_s or Tr of both leaves, even though it altered bleeding rates significantly. These results suggest a potentially more important role of root-sourced temperature signals than water signals on stomatal aperture under the conditions of our experiment. The effects of phytohormones in RZ temperature regulation should be investigated in related further studies.

The metabolic photosynthetic potential excluding stomatal limitation is reflected by V_{cmax} and J_{sat} estimated from the A-C_c curves [57]. The decline of V_{cmax} in S13 seedlings was consistent with the trend of Rubisco activity (Tables 2 and 3). Li et al. [58] reported decreases in both Rubisco content and activity in cucumber leaves under sub-optimal temperature conditions, which were ascribed to the H_2O_2- and glutathione-mediated cell redox state. Tezara et al. [59] demonstrated that under water stress, suppression of photosynthetic assimilation is mainly because the loss of ATP synthase (coupling factor) induces inhibition of ribulose bisphosphate synthesis, which determines J_{sat} [31]. Lack of ATP, or a decreased ATP/ADP ratio may also inactivate Rubisco-activase and then decrease Rubisco activity [60,61]. Notably, ATP synthase is preferentially attacked by singlet oxygen in a conditional mutant *flu* of *Arabidopsis* [62]. Thus, the source of the decline in metabolic potential could be the light reactions, where reactive oxygen species (ROS) will be generated once photoinhibition occurs.

At a sub-optimal air temperature 20/12°C, photosynthetic electron transport in the first leaf was greater in S19 than in S13 seedlings due to RZ warming (Fig 4). PSII function was improved by S19 (healthy TR_0/ABS and improved ET_0/TR_0; Fig 5B). Additionally, Φ_{NPQ} was not induced by the low air-temperature in either S13 or S19 seedlings, resulting in a higher proportion of Φ_{NO} in S13 than in S19 seedlings. The relatively high Φ_{NO} may lead to excess energy which will stimulate the generation of ROS [63,64]. Venzhik et al. [51] interpreted the reduced rate of electron transport in leaves of root-chilled seedlings as a result of adaptive transformations of the chloroplast membrane complex. This interpretation is consistent with our conditions, in which RZ warming may help mitigate such passive defence. Another aspect is nutrient condition. A cool RZ temperature may disturb the absorption of minerals such as N, Mg, Mn, and Zn [6,15], which are the core elements of the photosynthetic apparatus and antioxidant enzymes. In a newly unfolded leaf, this nutrient deficiency can be partially alleviated by decreasing its growth rate and receiving nutrients transferred from older tissues. This is a potential interpretation for the adaption occurring in the newly unfolded leaf.

The occurrence of PSI photoinhibition under both chilling and light intensity stress is an important feature in *Cucumis* plants [27,65]. However, in this experiment, the daytime air temperature (20°C) was higher than the level (10°C) below which PSI photoinhibition is usually observed. Moreover, the phenomenon of greater induction of Φ_{ND} rather than Φ_{NA} is also different from typical PSI photoinhibition. The increase in Φ_{ND} in S13 seedlings together with reduced RE_0/ET_0, which refers to the efficiency of electron movement from the PQ pool to the PSI end acceptors [44], suggests that electron transport between PQH_2 and cytochrome (cyt) b_6/f might have been partially blocked or bypassed under overall sub-optimal temperature environment. This phenomenon might be related to stimulated plastid activity of terminal

oxidase (PTOX), which has been suggested to act as a safety valve to prevent over-reduction of the electron transfer chain [66,67].

Although chilling or sub-optimal temperature-induced photoinhibition has been observed in various plant species [68–72], the interaction between RZ temperature and photosynthetic electron transport has rarely been further investigated. No consensus on RZ temperature effects has been achieved, possibly due to differences in evaluated species, treatment intensities or sampling location. For example, in wheat seedlings at an air temperature of 22°C, a 2°C RZ temperature decreased ETR_{II} and increased the coefficient of non-photochemical quenching (qN) [51]. In cucumber plants exposed to ambient air temperature in a study by Zhang et al. [50], a 14°C RZ temperature did not induce any photoinhibition. In rice seedlings at a chilling air temperature of 10°C, a 25°C warm root temperature severely blocked electron transport in leaves and led to visible damage [20]. In our preliminary experiment, a 23°C RZ temperature treatment performed poorly at 20/12°C sub-optimal air temperature and was abandoned. Although 20–25°C is considered an optimal temperature range for cucumber roots under ambient air temperature conditions [7,73], the definition of "optimal root temperature" should be adjusted once the shoot temperature is changed. The results described above indicate the complexity of shoots/roots interactions in plant responses to the surrounding temperature, and underline the necessity of specifying the air temperature when evaluating the effects of RZ temperature regulation.

Conclusion

Our results demonstrate that moderate RZ warming can increase RGR of cucumber seedlings under sub-optimal air temperature but does not influence new leaf emergence, leading to a reduced RGR compared with overall optimal temperature conditions. The promotion of growth by RZ warming consists of two different aspects in mature and newly unfolded leaves. In mature leaves, RZ warming substantially increases the net photosynthesis rate to the level measured under the optimal temperature condition by alleviating both diffusive and metabolic limitation. In the newly unfolded leaves, RZ warming significantly promotes leaf area expansion and reduces the stomatal limitation of photosynthesis. RZ warming also improved the root-sourced water supply, with a greater effect on new leaf expansion than on photosynthesis.

Supporting Information

S1 Fig. Typical daily air and root-zone temperature fluctuations in different treatments.
(TIF)

S1 Table. Chl fluorescence and the P700+ parameters in the second true leaves under different root-zone temperature and PEG treatments.
(DOCX)

S2 Table. The JIP-test results in the second true leaf of cucumber seedlings under different root-zone temperature and PEG treatments.
(DOCX)

Acknowledgments

Author Contributions

Conceived and designed the experiments: XW WZ LG. Performed the experiments: XW WZ YM. Analyzed the data: XW WZ. Wrote the paper: XW WZ LG.

References

1. Van Der Ploeg A, Heuvelink E. Influence of sub-optimal temperature on tomato growth and yield: a review. J Hortic Sci Biotechnol. 2005; 80(6):652–9. WOS:000233703500002.

2. Gao LH, Qu M, Ren HZ, Sui XL, Chen QY, Zhang ZX. Structure, function, application, and ecological benefit of a single-slope, energy-efficient solar greenhouse in China. Horttechnology. 2010; 20(3):626–31. WOS:000281497000027.

3. Jones DAG, Sandwell I, Talent CJW. The effect of soil temperature when associated with low air temperatures on the cropping of early tomatoes. Acta Hortic. 1978;(76:):167–71. BIOSIS: PREV197916031448.

4. Kawasaki Y, Matsuo S, Kanayama Y, Kanahama K. Effect of root-zone heating on root growth and activity, nutrient uptake, and fruit yield of tomato at low air temperatures. Engei Gakkai Zasshi. 2014; 83 (4):295–301. WOS:000343627500004.

5. Beyhan B, Paksoy H, Dasgan Y. Root zone temperature control with thermal energy storage in phase change materials for soilless greenhouse applications. Energy Convers Manag. 2013; 74:446–53. doi: 10.1016/j.enconman.2013.06.047 WOS:000325302700046.

6. Tachibana S. Comparison of effects of root temperature on the growth and mineral-nutrition of cucumber cultivars and figleaf gourd. Engei Gakkai Zasshi. 1982; 51(3):299–308. ISI:A1982PV35200007.

7. Lee SH, Singh AP, Chung GC, Ahn SJ, Noh EK, Steudle E. Exposure of roots of cucumber (*Cucumis sativus*) to low temperature severely reduces root pressure, hydraulic conductivity and active transport of nutrients. Physiol Plant. 2004; 120(3):413–20. doi: 10.1111/j.0031-9317.2004.00248.x PMID: 15032838.

8. Bigot J, Boucaud J. Low-temperature pretreatment of the root-system of brassica-rapa l plants—effects on the xylem sap exudation and on the nitrate absorption rate. Plant Cell Environ. 1994; 17(6):721–9. doi: 10.1111/j.1365-3040.1994.tb00164.x WOS:A1994NQ62100005.

9. Du YC, Tachibana S. Photosynthesis, photosynthate translocation and metabolism in cucumber roots held at supraoptimal temperature. Engei Gakkai Zasshi. 1994; 63(2):401–8. ISI:A1994PH97200020.

10. Poire R, Schneider H, Thorpe MR, Kuhn AJ, Schurr U, Walter A. Root cooling strongly affects diel leaf growth dynamics, water and carbohydrate relations in *Ricinus communis*. Plant Cell Environ. 2010; 33 (3):408–17. doi: 10.1111/j.1365-3040.2009.02090.x PMID: 19968824.

11. Delucia EH, Heckathorn SA, Day TA. Effects of soil temperature on growth, biomass allocation and resource acquisition of *Andropogon gerardii* Vitman. New Phytol. 1992; 120(4):543–9. doi: 10.1111/j.1469-8137.1992.tb01804.x

12. He J, Lee SK, Dodd IC. Limitations to photosynthesis of lettuce grown under tropical conditions: alleviation by root-zone cooling. J Exp Bot. 2001; 52(359):1323–30. doi: 10.1093/jexbot/52.359.1323 WOS:000169877400019. PMID: 11432951

13. Lee JW, Lee EH, Kim KD, Lee WS. Effects of root-zone warming on fruit enlargement and yield of cucumber grown in a greenhouse. Journal of the Korean Society for Horticultural Science. 2003; 44 (5):639–43. BIOSIS:PREV200400022460.

14. Wan XC, Landhausser SM, Zwiazek JJ, Lieffers VJ. Stomatal conductance and xylem sap properties of aspen (*Populus tremuloides*) in response to low soil temperature. Physiol Plant. 2004; 122(1):79–85. doi: 10.1111/j.1399-3054.2004.00385.x WOS:000223589000010.

15. Tachibana S. Effect of root temperature on the rate of water and nutrient absorption in cucumber cultivars and figleaf gourd. Engei Gakkai Zasshi. 1987; 55(4):461–7. ISI:A1987G585100007.

16. Lee SH, Chung GC, Steudle E. Gating of aquaporins by low temperature in roots of chilling-sensitive cucumber and chilling-tolerant figleaf gourd. J Exp Bot. 2005; 56(413):985–95. doi: 10.1093/jxb/eri092 PMID: 15734792.

17. Murai-Hatano M, Kuwagata T, Sakurai J, Nonami H, Ahamed A, Nagasuga K, et al. Effect of low root temperature on hydraulic conductivity of rice plants and the possible role of aquaporins. Plant Cell Physiol. 2008; 49(9):1294–305. doi: 10.1093/pcp/pcn104 WOS:000259205900004. PMID: 18676378

18. Dodd IC, He J, Turnbull CGN, Lee SK, Critchley C. The influence of supra-optimal root-zone temperatures on growth and stomatal conductance in *Capsicum annuum* L. J Exp Bot. 2000; 51(343):239–48. doi: 10.1093/jexbot/51.343.239 WOS:000085380200010. PMID: 10938830

19. Suzuki K, Nagasuga K, Okada M. The chilling injury induced by high root temperature in the leaves of rice seedlings. Plant Cell Physiol. 2008; 49(3):433–42. doi: 10.1093/pcp/pcn020 WOS:000254004500013. PMID: 18252732

20. Suzuki K, Ohmori Y, Ratel E. High root temperature blocks both linear and cyclic electron transport in the dark during chilling of the leaves of rice seedlings. Plant Cell Physiol. 2011; 52(9):1697–707. doi: 10.1093/pcp/pcr104 PMID: 21803813

21. Soto A, Hernandez L, Quiles MJ. High root temperature affects the tolerance to high light intensity in *Spathiphyllum* plants. Plant Sci. 2014; 227:84–9. doi: 10.1016/j.plantsci.2014.07.004 WOS:000342865000011. PMID: 25219310

22. Paredes M, Quiles MJ. The Effects of Cold Stress on Photosynthesis in Hibiscus Plants. PLoS One. 2015; 10(9):13. doi: 10.1371/journal.pone.0137472 WOS:000361043100042.

23. Hao HP, Jiang CD, Zhang SR, Tang YD, Shi L. Enhanced thermal-tolerance of photosystem II by elevating root zone temperature in *Prunus mira* Koehne seedlings. Plant Soil. 2011:1–12. doi: 10.1007/s11104-011-1037-y

24. Xu WF, Jia LG, Shi WM, Liang JS, Zhou F, Li QF, et al. Abscisic acid accumulation modulates auxin transport in the root tip to enhance proton secretion for maintaining root growth under moderate water stress. New Phytol. 2013; 197(1):139–50. doi: 10.1111/nph.12004 WOS:000311606800017. PMID: 23106247

25. Zhou YH, Lam HM, Zhang JH. Inhibition of photosynthesis and energy dissipation induced by water and high light stresses in rice. J Exp Bot. 2007; 58(5):1207–17. doi: 10.1093/jxb/erl291 WOS:000246208900030. PMID: 17283375

26. Bulder HAM, Vanderleij WR, Speek EJ, Vanhasselt PR, Kuiper PJC. Interactions of drought and low-temperature stress on lipid and fatty-acid composition of cucumber genotypes differing in growth-response at suboptimal temperature. Physiol Plant. 1989; 75(3):362–8. doi: 10.1111/j.1399-3054.1989.tb04639.x WOS:A1989T719700007.

27. Terashima I, Noguchi K, Itoh-Nemoto T, Park YM, Kubo A, Tanaka K. The cause of PSI photoinhibition at low temperatures in leaves of *Cucumis sativus*, a chilling-sensitive plant. Physiol Plant. 1998; 103(3):295–303. doi: 10.1034/j.1399-3054.1998.1030301.x WOS:000075545800001.

28. Yamazaki K. Yōeki saibai zenpen. Tokyo: Hakuyūsha; 1982.

29. Choi KJ, Chung GC, Choi WY, Han KP, Choi SK. Effect of root zone temperatures on the mineral composition of xylem sap, photosynthetic activity and transpiration in cucumber plants. Hydroponics and Transplant Production. 1995;(396:):161–6. WOS:000071637900018.

30. Hunt R. Plant growth analysis. London: Edward Arnold (Publishers) Ltd.; 1978.

31. Sharkey TD, Bernacchi CJ, Farquhar GD, Singsaas EL. Fitting photosynthetic carbon dioxide response curves for C3 leaves. Plant Cell Environ. 2007; 30(9):1035–40. PMID: 17661745

32. Jin SH, Huang JQ, Li XQ, Zheng BS, Wu JS, Wang ZJ, et al. Effects of potassium supply on limitations of photosynthesis by mesophyll diffusion conductance in *Carya cathayensis*. Tree Physiol. 2011; 31(10):1142–51. doi: 10.1093/treephys/tpr095 WOS:000295930200010. PMID: 21990026

33. Farquhar GD, Sharkey TD. Stomatal Conductance and Photosynthesis. Annu Rev Plant Biol. 1982; 33(1):317–45. doi: 10.1146/annurev.pp.33.060182.001533

34. Sartory D, Grobbelaar J. Extraction of chlorophyll a from freshwater phytoplankton for spectrophotometric analysis. Hydrobiologia. 1984; 114(3):177–87.

35. Zhang L, Zhang L, Sun J, Zhang Z, Ren H, Sui X. Rubisco gene expression and photosynthetic characteristics of cucumber seedlings in response to water deficit. Sci Hortic. 2013; 161:81–7.

36. Bradford MM. A rapid and sensitive method for the quantitation of microgram quantities of protein utilizing the principle of protein-dye binding. Anal Biochem. 1976; 72(1–2):248–54. doi: 10.1016/0003-2697(76)90527-3

37. Sun JL, Sui XL, Wang SH, Wei YX, Huang HY, Hu LP, et al. The response of *rbcL*, *rbcS* and *rca* genes in cucumber (*Cucumis sativus* L.) to growth and induction light intensity. Acta Physiol Plant. 2014; 36(10):2779–91. doi: 10.1007/s11738-014-1648-z WOS:000342412100021.

38. Pfündel E, Klughammer C, Schreiber U. Monitoring the effects of reduced PSII antenna size on quantum yields of photosystems I and II using the Dual-PAM-100 measuring system. PAM Application Notes. 2008; 1:21–4.

39. Kramer D, Johnson G, Kiirats O, Edwards G. New fluorescence parameters for the determination of QA redox state and excitation energy fluxes. Photosynth Res. 2004; 79(2):209–18. doi: 10.1023/B:PRES.0000015391.99477.0d PMID: 16228395

40. Klughammer C, Schreiber U. Complementary PS II quantum yields calculated from simple fluorescence parameters measured by PAM fluorometry and the Saturation Pulse method. PAM Application Notes. 2008; 1:27–35.

41. Klughammer C, Schreiber U. Saturation pulse method for assessment of energy conversion in PS I. PAM Application Notes. 2008; 1:11–4. Epub 14.

42. Strasser RJ, Tsimilli-Michael M, Qiang S, Goltsev V. Simultaneous in vivo recording of prompt and delayed fluorescence and 820-nm reflection changes during drying and after rehydration of the resurrection plant Haberlea rhodopensis. Biochim Biophys Acta. 2010; 1797(6–7):1313–26. doi: 10.1016/j. bbabio.2010.03.008 PMID: 20226756

43. Strasser RJ, Tsimilli-Michael M, Srivastava A. Analysis of the chlorophyll a fluorescence transient. In: Papageorgiou GC, Govindjee X, editors. Chlorophyll Fluorescence: a Signature of Photosynthesis. Dordrecht: Springer Netherlands; 2004. pp. 321–362.

44. Strasser RJ, Tsimilli-Michael M, Qiang S, Goltsev V. Simultaneous in vivo recording of prompt and delayed fluorescence and 820-nm reflection changes during drying and after rehydration of the resurrection plant *Haberlea rhodopensis*. Biochim Biophys Acta. 2010; 1797(6–7):1313–26. doi: 10.1016/j. bbabio.2010.03.008 WOS:000279663200087. PMID: 20226756

45. Paul EMM, Hardwick RC, Parker PF. Genotypic variation in the response to suboptimal temperatures of growth in tomato (*Lycopersicon-esculentum* Mill). New Phytol. 1984; 98(2):221–30. doi: 10.1111/j. 1469-8137.1984.tb02732.x WOS:A1984TU48600002.

46. Nie GY, Long SP, Baker NR. The effects of development at suboptimal growth temperatures on photosynthetic capacity and susceptibility to chilling-dependent photoinhibition in *Zea-mays*. Physiol Plant. 1992; 85(3):554–60. doi: 10.1111/j.1399-3054.1992.tb05826.x WOS:A1992JH73500022.

47. Kuwagata T, Ishikawa-Sakurai J, Hayashi H, Nagasuga K, Fukushi K, Ahamed A, et al. Influence of low air humidity and low root temperature on water uptake, growth and aquaporin expression in rice plants. Plant Cell Physiol. 2012; 53(8):1418–31. doi: 10.1093/pcp/pcs087 WOS:000307834200006. PMID: 22685088

48. Ahn SJ, Im YJ, Chung GC, Cho BH, Suh SR. Physiological responses of grafted-cucumber leaves and rootstock roots affected by low root temperature. Sci Hortic. 1999; 81(4):397–408. doi: 10.1016/S0304-4238(99)00042-4 WOS:000083123800002.

49. Adebooye OC, Schmitz-Eiberger M, Lankes C, Noga GJ. Inhibitory effects of sub-optimal root zone temperature on leaf bioactive components, photosystem II (PS II) and minerals uptake in *Trichosanthes cucumerina* L. Cucurbitaceae. Acta Physiol Plant. 2010; 32(1):67–73. doi: 10.1007/s11738-009-0379-z WOS:000274654900009.

50. Zhang YP, Qiao YX, Zhang YL, Zhou YH, Yu JQ. Effects of root temperature on leaf gas exchange and xylem sap abscisic acid concentrations in six Cucurbitaceae species. Photosynthetica. 2008; 46 (3):356–62. ISI:000259257300006.

51. Venzhik YV, Titov AF, Talanova VV, Miroslavov EA. Ultrastructure and functional activity of chloroplasts in wheat leaves under root chilling. Acta Physiol Plant. 2014; 36(2):323–30. doi: 10.1007/ s11738-013-1413-8 WOS:000330805300009.

52. Strand A, Hurry V, Henkes S, Huner N, Gustafsson P, Gardestrom P, et al. Acclimation of Arabidopsis leaves developing at low temperatures. Increasing cytoplasmic volume accompanies increased activities of enzymes in the Calvin cycle and in the sucrose-biosynthesis pathway. Plant Physiol. 1999; 119 (4):1387–97. doi: 10.1104/pp.119.4.1387 WOS:000079737900026. PMID: 10198098

53. Kim T-H, Böhmer M, Hu H, Nishimura N, Schroeder JI. Guard Cell Signal Transduction Network: Advances in Understanding Abscisic Acid, CO_2, and Ca^{2+} Signaling. Annu Rev Plant Biol. 2010; 61 (1):561–91. doi: 10.1146/annurev-arplant-042809-112226

54. Schroeder JI, Allen GJ, Hugouvieux V, Kwak JM, Waner D. Guard cell signal transduction. Annu Rev Plant Physiol Plant Mol Biol. 2001; 52(1):627–58. doi: 10.1146/annurev.arplant.52.1.627

55. Rogiers SY, Clarke SJ. Nocturnal and daytime stomatal conductance respond to root-zone temperature in 'Shiraz' grapevines. Ann Bot. 2013; 111(3):433–44. doi: 10.1093/aob/mcs298 WOS:000316691800011. PMID: 23293018

56. Ntatsi G, Savvas D, Huntenburg K, Druege U, Hincha DK, Zuther E, et al. A study on ABA involvement in the response of tomato to suboptimal root temperature using reciprocal grafts with notabilis, a null mutant in the ABA-biosynthesis gene LeNCED1. Environ Exp Bot. 2014; 97:11–21. doi: 10.1016/j. envexpbot.2013.09.011 WOS:000327916000002.

57. von Caemmerer S. Steady-state models of photosynthesis. Plant Cell Environ. 2013; 36(9):1617–30. doi: 10.1111/pce.12098 WOS:000322709300006. PMID: 23496792

58. Li H, Wang XM, Chen L, Ahammed GJ, Xia XJ, Shi K, et al. Growth temperature-induced changes in biomass accumulation, photosynthesis and glutathione redox homeostasis as influenced by hydrogen peroxide in cucumber. Plant Physiol Biochem. 2013; 71:1–10. doi: 10.1016/j.plaphy.2013.06.018 WOS:000325836600001. PMID: 23860263

59. Tezara W, Mitchell VJ, Driscoll SD, Lawlor DW. Water stress inhibits plant photosynthesis by decreasing coupling factor and ATP. Nature. 1999; 401(6756):914–7. WOS:000083464700058.

60. Lawlor DW, Tezara W. Causes of decreased photosynthetic rate and metabolic capacity in water-deficient leaf cells: a critical evaluation of mechanisms and integration of processes. Ann Bot. 2009; 103 (4):561–79. doi: 10.1093/aob/mcn244 WOS:000263162300003. PMID: 19155221

61. Parry MAJ, Andralojc PJ, Khan S, Lea PJ, Keys AJ. Rubisco activity: effects of drought stress. Ann Bot. 2002; 89(7):833–9. doi: 10.1093/aob/mcf103

62. Mahler H, Wuennenberg P, Linder M, Przybyla D, Zoerb C, Landgraf F, et al. Singlet oxygen affects the activity of the thylakoid ATP synthase and has a strong impact on its gamma subunit. Planta. 2007; 225 (5):1073–83. doi: 10.1007/s00425-006-0416-8 WOS:000245006500002. PMID: 17103225

63. Klughammer C, Schreiber U. Complementary PS II quantum yields calculated from simple fluorescence parameters measured by PAM fluorometry and the Saturation Pulse method. PAM Application Notes. 2008; 1:27–35.

64. Miller G, Suzuki N, Ciftci-Yilmaz S, Mittler R. Reactive oxygen species homeostasis and signalling during drought and salinity stresses. Plant Cell Environ. 2010; 33(4):453–67. doi: 10.1111/j.1365-3040. 2009.02041.x WOS:000275146200001. PMID: 19712065

65. Sonoike K. Photoinhibition of photosystem I. Physiol Plant. 2011; 142(1):56–64. doi: 10.1111/j.1399-3054.2010.01437.x WOS:000289470800007. PMID: 21128947

66. Peltier G, Cournac L. Chlororespiration. Annual Review of Plant Biology. 2002; 53:523–50. doi: 10.1146/annurev.arplant.53.100301.135242 WOS:000177183300022. PMID: 12227339

67. Rumeau D, Peltier G, Cournac L. Chlororespiration and cyclic electron flow around PSI during photosynthesis and plant stress response. Plant Cell and Environment. 2007; 30(9):1041–51. doi: 10.1111/j. 1365-3040.2007.01675.x WOS:000248791000002.

68. Zhang YJ, Yang JS, Guo SJ, Meng JJ, Zhang YL, Wan SB, et al. Over-expression of the *Arabidopsis* CBF1 gene improves resistance of tomato leaves to low temperature under low irradiance. Plant Biol. 2011; 13(2):362–7. doi: 10.1111/j.1438-8677.2010.00365.x ISI:000287198800016. PMID: 21309983

69. Sonoike K. The different roles of chilling temperatures in the photoinhibition of photosystem I and photosystem II. J Photochem Photobiol B. 1999; 48(2–3):136–41. doi: 10.1016/s1011-1344(99)00030-5

70. Liang Y, Chen H, Tang MJ, Yang PF, Shen SH. Responses of *Jatropha curcas* seedlings to cold stress: photosynthesis-related proteins and chlorophyll fluorescence characteristics. Physiol Plant. 2007; 131 (3):508–17. doi: 10.1111/j.1399-3054.2007.00974.x WOS:000249827100014. PMID: 18251888

71. Fracheboud Y, Haldimann P, Leipner J, Stamp P. Chlorophyll fluorescence as a selection tool for cold tolerance of photosynthesis in maize (*Zea mays* L.). J Exp Bot. 1999; 50(338):1533–40. doi: 10.1093/jexbot/50.338.1533 WOS:000082662300013.

72. Huner NPA, Oquist G, Sarhan F. Energy balance and acclimation to light and cold. Trends Plant Sci. 1998; 3(6):224–30. WOS:000074048200008.

73. Zhang YP, Jia FF, Zhang XM, Qiao YX, Shi K, Zhou YH, et al. Temperature effects on the reactive oxygen species formation and antioxidant defence in roots of two cucurbit species with contrasting root zone temperature optima. Acta Physiol Plant. 2012; 34(2):713–20. doi: 10.1007/s11738-011-0871-0 WOS:000300453500031.